Supporting Information

Efficient Thermally Activated Delayed Fluorescent Emitter Based on Spiro-typed Benzo[b]acridine Donor and Benzophenone Acceptor

Xiangan Song[a], Zhangshan Liu[b], Mengyao Lu[a], Shengnan Zou[a], Fengyun Guo[a], Shiyong Gao[a], Zujin Zhao[b]*, Ben Zhong Tang[c], Yong Zhang[a,d]*

[a]School of Materials Science and Engineering, Harbin Institute of Technology, Harbin 150001, China. E-mail: yongzhang@hit.edu.cn

[b]State Key Laboratory of Luminescent Materials and Devices, Guangdong Provincial Key Laboratory of Luminescence from Molecular Aggregates, South China University of Technology, Guangzhou 510640, China. E-mail: mszjzhao@scut.edu.cn

[c]School of Science and Engineering, Shenzhen Institute of Aggregate Science and Technology, The Chinese University of Hong Kong, Shenzhen, Guangdong 518172, China.

[d]Key Laboratory of Opto-electronic Chemical Materials and Devices, Ministry of Education, Jianghan University, Wuhan, 430056, China

Contents

1. General Information

All regents and solvents used for the synthesis of the compound were purchased from commercial source and used without further purification.

2. Electrochemical Characterization

The oxidation potential was determined by cyclic voltammetry using 0.1 M tetrabutylammonium hexafluorophosphate ($TBAPF_6$) in CH_2Cl_2 (CV) as a supporting electrolyte and a scan rate of 100 mV s^{-1}. ITO, Ag/AgCl and Pt mesh were used as working electrode, reference electrode and counter electrode, respectively. A 3-electrode cell comprising silver/silver chloride (Ag/AgCl), a platinum mesh and ITO as the reference, counter, and working electrodes, respectively, were used. All potentials were recorded versus Ag/AgCl (saturated) as a reference electrode. Oxidation of the ferrocene/ferrocenium (Fc/Fc^+) redox couple in $CH_2Cl_2/TBAPF_6$ occurs at E_o = + 0.48 V. HOMO levels were conducted from the oxidation half-wave potential with the formula: E_{HOMO} = - ($E_{oxi.\ v.s.\ Fc+/Fc}$ + 4.8) (eV), $E_{LUMO} = E_{HOMO} + E_g$, thereinto, E_g was obtained from the absorption edges of normalized absorption spectra.

3. Photophysical Characterization

Absorption spectra were studied using a UV-vis-NIR spectrophotometer (UV-1650 PC, Shimadzu). Photoluminescence (PL) spectra and phosphorescence spectra were performed at 77 K using a HITACHI F-4600 spectrophotometer. The transient photoluminance decay characteristics were measured using an Edinburgh Instruments FLS920 spectrometer. The temperature dependence experiment is conducted under low temperature refrigeration system from Advanced Research Systems Company. The absolute fluorescence quantum yields of the solid films are measured with an integrating sphere.

4. OLED Fabrication and Characterization

The glass substrates precoated with a 90 nm layer of indium tin oxide (ITO) with a sheet resistance of 15 ~ 20 Ω per square were successively cleaned in ultrasonic bath of acetone, isopropanol, detergent and deionized water, respectively, taking 10 min for each step. Then, the substrates were totally dried in a 70 ℃ oven. Before the fabrication processes, in order to improve the hole injection ability of ITO, the substrates were treated by O_2 plasma for 10 min. The vacuum-deposited OLEDs were fabricated under a pressure of less than 5×10^{-4} Pa in the Fangsheng OMV-FS380 vacuum deposition system. Organic materials, LiF and Al were deposited at rates of 1 ~ 2 A s^{-1}, 0.1 A s^{-1} and 5 A s^{-1}, respectively. The effective emitting area of the devices was 9 mm^2, determined by the overlap between anode and cathode. The luminance–voltage–current density characteristics and EL spectra were obtained via a Konica Minolta CS-200 Color and Luminance Meter and an Ocean Optics USB 2000 + spectrometer, along with a Keithley 2400 Source Meter. The external quantum efficiencies were estimated utilizing the normalized EL spectra and the current efficiencies of the devices, assuming that the devices are Lambertian emitters. All the characterizations were conducted at room temperature in ambient conditions without any encapsulation, as soon as the devices were fabricated.

5. Quantum Chemical Calculations

The ground state structures were optimized using the Gaussian 09 program package. The electron density distribution of frontier molecular orbital (FMO) were visualized with Gaussview 5.0. Structure optimizations were carried out using density functional

theory (DFT) calculations. The ground state structures were optimized with B3LYP/6-31G(d) level set in the gas phase. Natural transition orbital (NTO) analysis for the S1 and Tm (m=1-3) states are analyzed at the PBE0/6-31G(d) level and visualized with Multiwfn 3.8[1] an VMD 1.9.3[2]. The spin-orbital coupling (SOC) was also calculated by the TD-DFT method at the PBE0/def2-tzvp level using ORCA 5.0 software package. Please refer to the supporting information for more details.

6. Synthesis Procedures

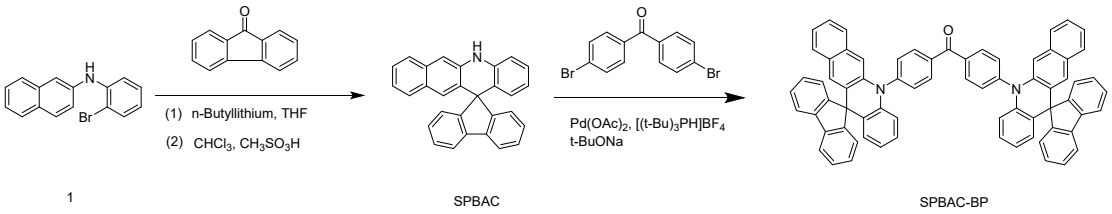

Scheme S1. Synthetic routes of SPBAC-BP

Synthesis of 5H-spiro[benzo[b]acridine-12,9'-fluorene] (SPBAC): To a solution of 1 (8.6 g, 29.1 mmol) in dry THF (150 mL), n-BuLi (2.5 M in hexane, 25.6 mL, 64.0 mmol) was added dropwise at -78°C. After stirring for 2 h, fluorenone (5.76 g, 110.00 mmol) was added as a solution while stirring the solution at -78°C for 30 min. The reaction mixture was allowed to warm to room temperature and stirred for overnight. After quenching by a large amount of water, the resulting mixture was extracted three with $CHCl_2$. A combined $CHCl_2$ solution was dried over anhydrous $MgSO_4$ and concentrated to afford a hydroxy intermediate, after filtration and evaporation. The crude hydroxyl intermediate was dissolved in $CHCl_3$ (150 mL), and methane sulfonic acid (6.15 g, 64.02 mmol) was added and then refluxed for 10 h. After cooling to room temperature, the resulting solution was carefully poured into an excess amount of $NaHCO_3$ aqueous solution and stirred for 20 min. The product was extracted by $CHCl_2$, dried over anhydrous $MgSO_4$. After filtration and evaporation, the crude product was purified by column chromatography on silica gel (hexane/CH_2Cl_2 = 4:1, v/v) filtered off, and then dried under reduced pressure to afford SPBAC as a white solid (yield = 4.2 g, 39%). ^{1}H NMR (400 MHz, DMSO) δ 9.40 (s, 1H), 8.05 (d, J = 7.6 Hz, 2H), 7.72 (d, J = 8.8 Hz, 1H), 7.59 (d, J = 8.0 Hz, 1H), 7.37 (t, J = 7.3 Hz, 2H), 7.28 (d, J = 8.8 Hz, 1H), 7.20 – 7.08 (m, 4H), 6.99 – 6.85 (m, 3H), 6.65 (t, J = 7.9 Hz, 1H), 6.51 (d, J = 8.8 Hz, 1H), 6.38 (t, J = 7.5 Hz, 1H), 5.95 (d, J = 8.0 Hz, 1H). ^{13}C NMR (151 MHz, DMSO) δ 158.27, 138.97, 138.43, 137.45, 132.39, 130.10, 129.94, 129.07,

128.93, 127.98, 127.85, 127.30, 126.06, 125.68, 123.85, 123.62, 121.91, 121.03, 120.19, 118.28, 114.64, 110.42.

Synthesis of bis(4-(5H-spiro[benzo[b]acridine-12,9'-fluoren]-5-yl)phenyl) methanone (SPBAC-BP): A mixture of 4,4′ -dibromobenzophenone (0.8 g, 2.5 mmol), SPBAC (1.9 g, 5 mmol), $Pd(OAc)_2$ (22.4 mg, 0.1 mmol), $[(t\text{-}Bu)_3PH]BF_4$ (115 mg, 0.4 mmol) and t-BuONa (1 g, 10 mmol) was added in 250 mL two-neck bottle under nitrogen. Then, adding 100 mL toluene into the bottle and the reaction mixture was refluxed for 12 h. After cooling to room temperature, the product was extracted by $CHCl_2$, dried over anhydrous $MgSO_4$. After filtration and evaporation, the crude product was purified by column chromatography on silica gel (hexane/CH_2Cl_2 = 2:1, v/v) filtered off, and then dried under reduced pressure to afford SPBAC-BP as a yellow solid (yield = 2.8 g, 60%). ^1H NMR (400 MHz, $CDCl_3$) δ 8.31 (d, J = 8.3 Hz, 4H), 7.94 (d, J = 7.6 Hz, 4H), 7.76 – 7.71 (m, 4H), 7.57 – 7.51 (m, 4H), 7.43 – 7.33 (m, 8H), 7.19 (td, J = 7.4, 1.1 Hz, 4H), 7.01 (ddd, J = 7.9, 6.7, 1.1 Hz, 2H), 6.87 – 6.82 (m, 4H), 6.82 – 6.75 (m, 4H), 6.51 (ddd, J = 8.1, 7.0, 1.2 Hz, 2H), 6.32 (ddd, J = 20.1, 8.2, 1.3 Hz, 4H). ^{13}C NMR (151 MHz, $CDCl_3$) δ 194.91, 158.29, 146.44, 139.31, 139.17, 138.98, 137.13, 133.05, 132.03, 129.93, 129.49, 128.70, 128.65, 128.46, 127.49, 126.70, 126.26, 125.63, 125.19, 124.85, 122.85, 121.26, 120.39, 117.19, 114.99, 114.08. HR-MS ($C_{71}H_{44}N_2O$): calcd for $C_{71}H_{44}N_2O$ (M) 940.15, found: 940.3468.

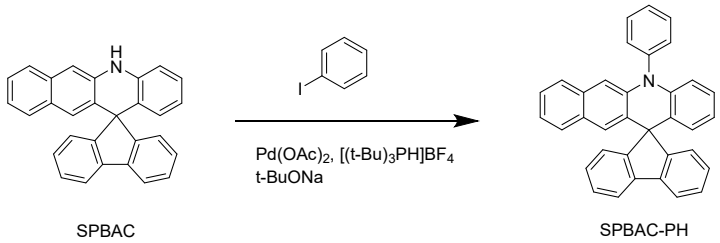

Scheme S2. Synthetic routes of SPBAC-PH

Synthesis of 5-phenyl-5H-spiro[benzo[b]acridine-12,9'-fluorene] (SPBAC-PH): A mixture of iodobenzene (1 g, 5 mmol), SPBAC (1.9 g, 5 mmol), $Pd(OAc)_2$ (22.4 mg, 0.1 mmol), $[(t\text{-}Bu)_3PH]BF_4$ (115 mg, 0.4 mmol) and t-BuONa (1 g, 10 mmol) was added in 250 mL two-neck bottle under nitrogen. Then, adding 100 mL toluene into the bottle and the reaction mixture was refluxed for 12 h. After cooling to room temperature, the product was extracted by $CHCl_2$, dried over anhydrous $MgSO_4$. After

filtration and evaporation, the crude product was purified by column chromatography on silica gel (hexane/CH_2Cl_2 = 4:1, v/v) filtered off, and then dried under reduced pressure to afford SPBAC-BP as a yellow solid (yield = 1.5 g, 65%). ^{1}H NMR (400MHz, $CDCl_3$) δ 7.92 (d, J = 7.6 Hz, 2H), 7.70 (td, J = 7.8, 1.4 Hz, 2H), 7.59 – 7.54 (m, 1H), 7.48 (dd, J = 19.6, 8.4 Hz, 4H), 7.36 (dd, J = 17.7, 7.5 Hz, 4H), 7.17 (t, J = 7.4 Hz, 2H), 6.97 (t, J = 7.3 Hz, 1H), 6.83 – 6.70 (m, 4H), 6.45 (t, J = 7.5 Hz, 1H), 6.25 (t, J = 7.7 Hz, 2H). ^{13}C NMR (151 MHz, $CDCl_3$) δ 158.50, 141.96, 139.85, 139.50, 139.11, 132.04, 131.51, 131.21, 129.74, 129.21, 128.64, 128.50, 128.38, 127.34, 126.52, 126.03, 125.70, 124.90, 124.75, 122.48, 120.74, 120.27, 117.40, 115.12, 113.49.

7. Supplementary Figures

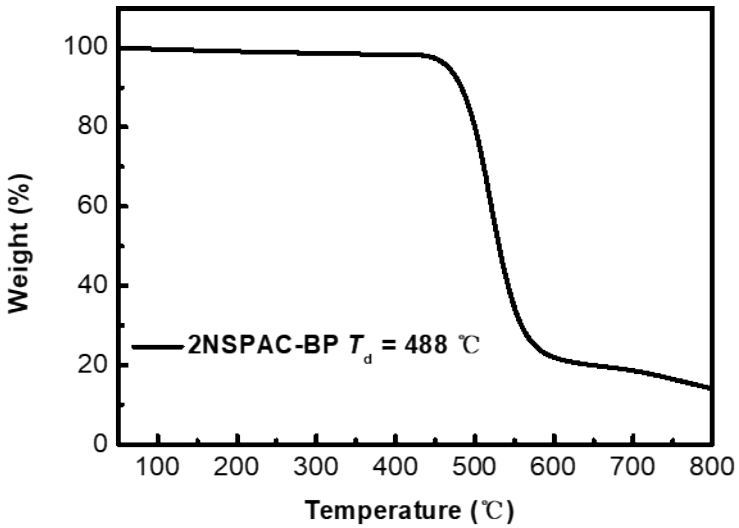

Figure S1 TGA measurements of **2NSPBAC—BP.**

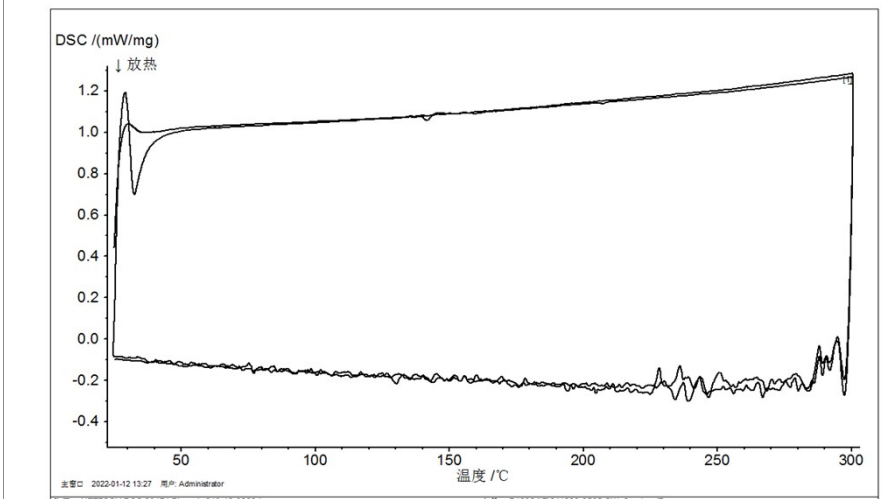

Figure S2 DSC measurements of **2NSPBAC—BP.**

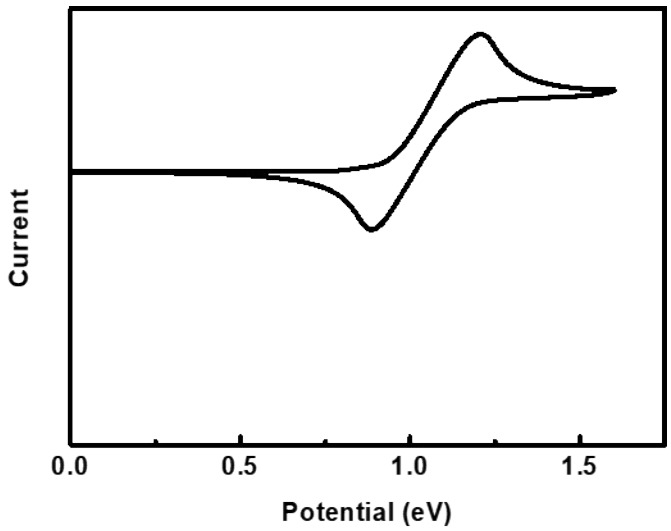

Figure S3 Cyclic voltammograms of **2NSPBAC--BP** in dichloromethane (DCM).

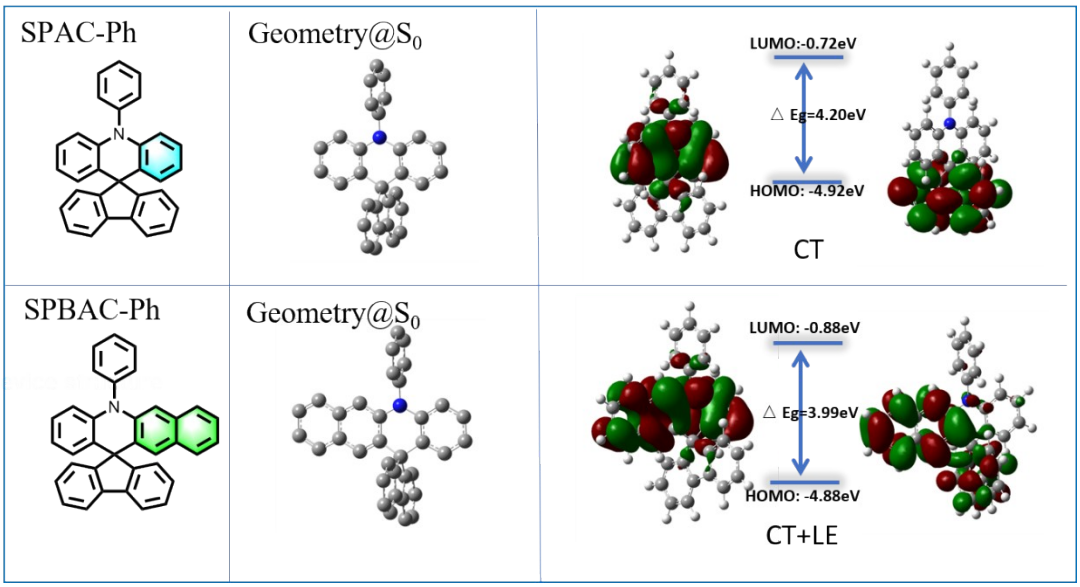

Figure S4 Calculated frontier orbital distributions of **SPAC--Ph** and **SPBAC--Ph**.

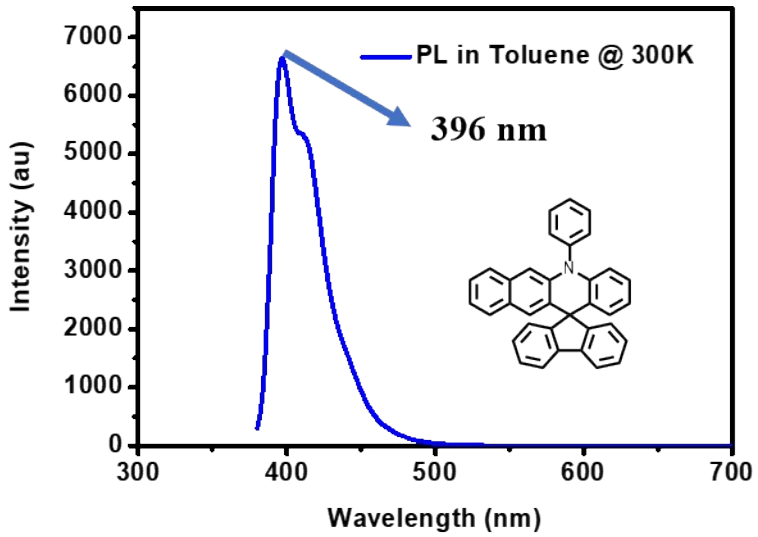

Figure S5 Fluorescence (300 K) spectra of **2NSPBAC-BP** in toluene.

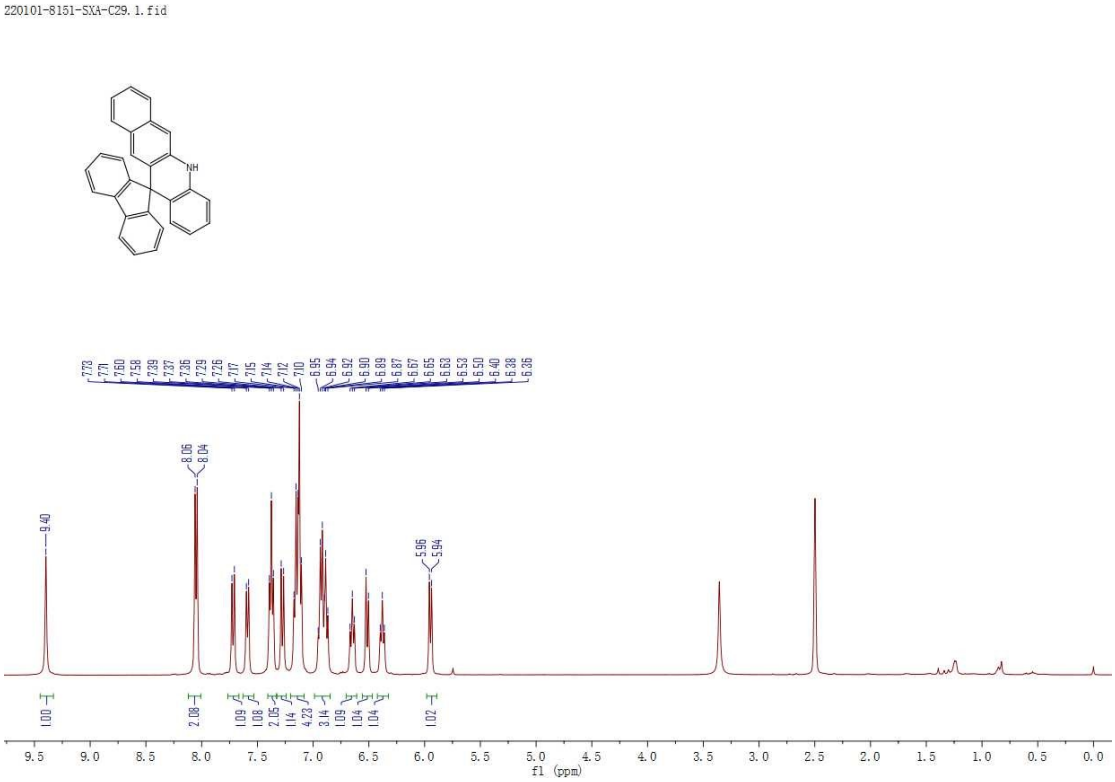

Figure S6 ^{1}H NMR spectrum of SPBAC (400 MHz, DMSO, 25 °C).

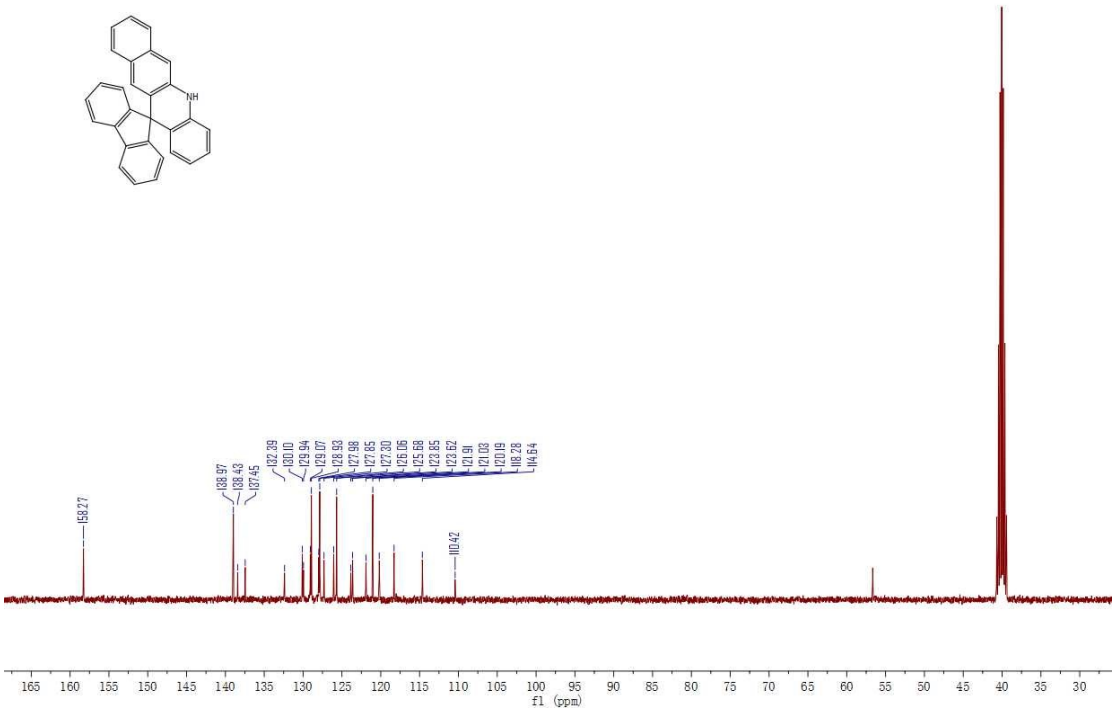

Figure S7 ^{13}C NMR spectrum of SPBAC (400 MHz, DMSO, 25 °C).

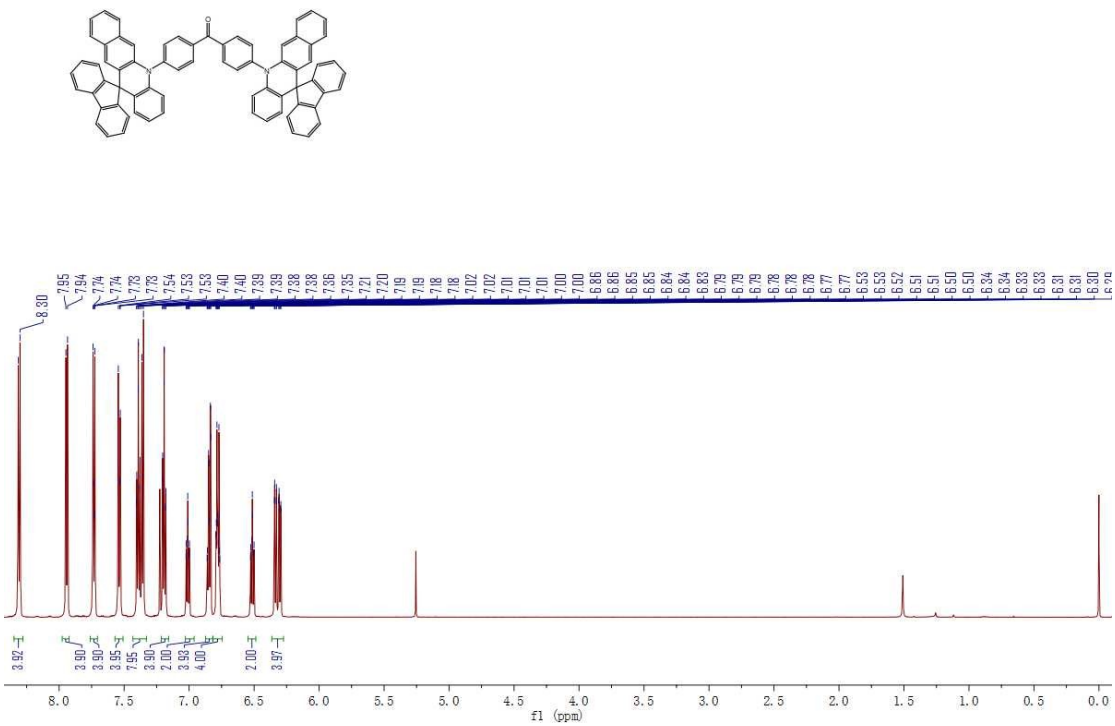

Figure S8 ^{1}H NMR spectrum of SPBAC-BP (400 MHz, $CDCl_3$, 25 °C).

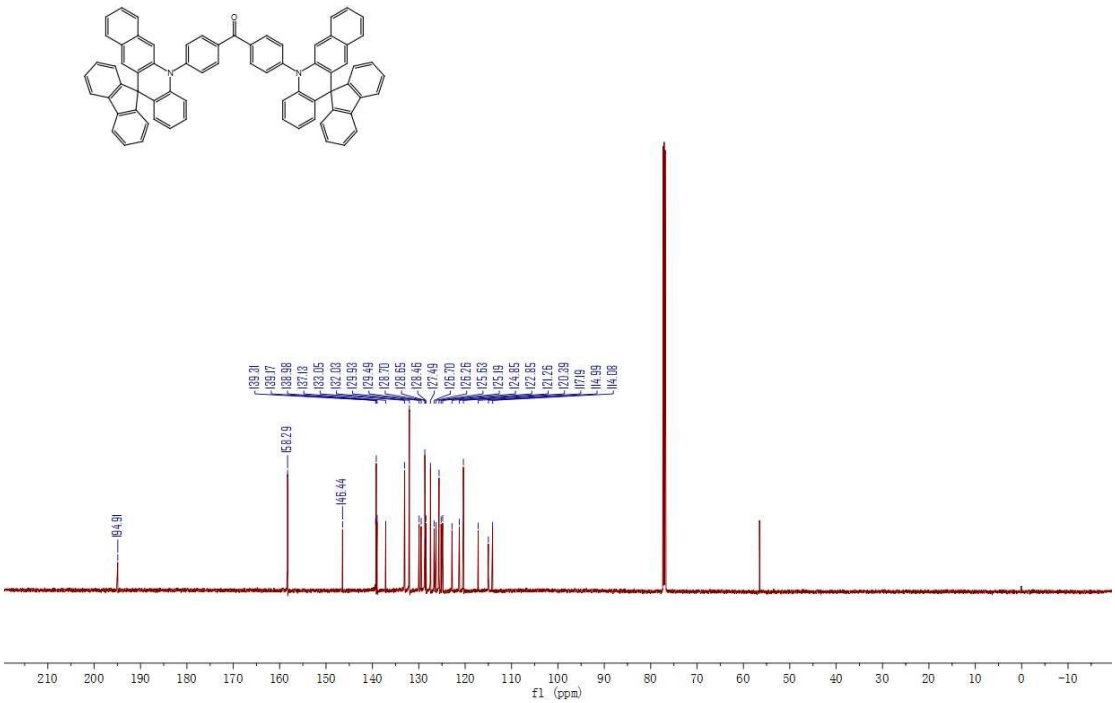

Figure S9 ^{13}C NMR spectrum of SPBAC-BP (400 MHz, $CDCl_3$, 25 °C).

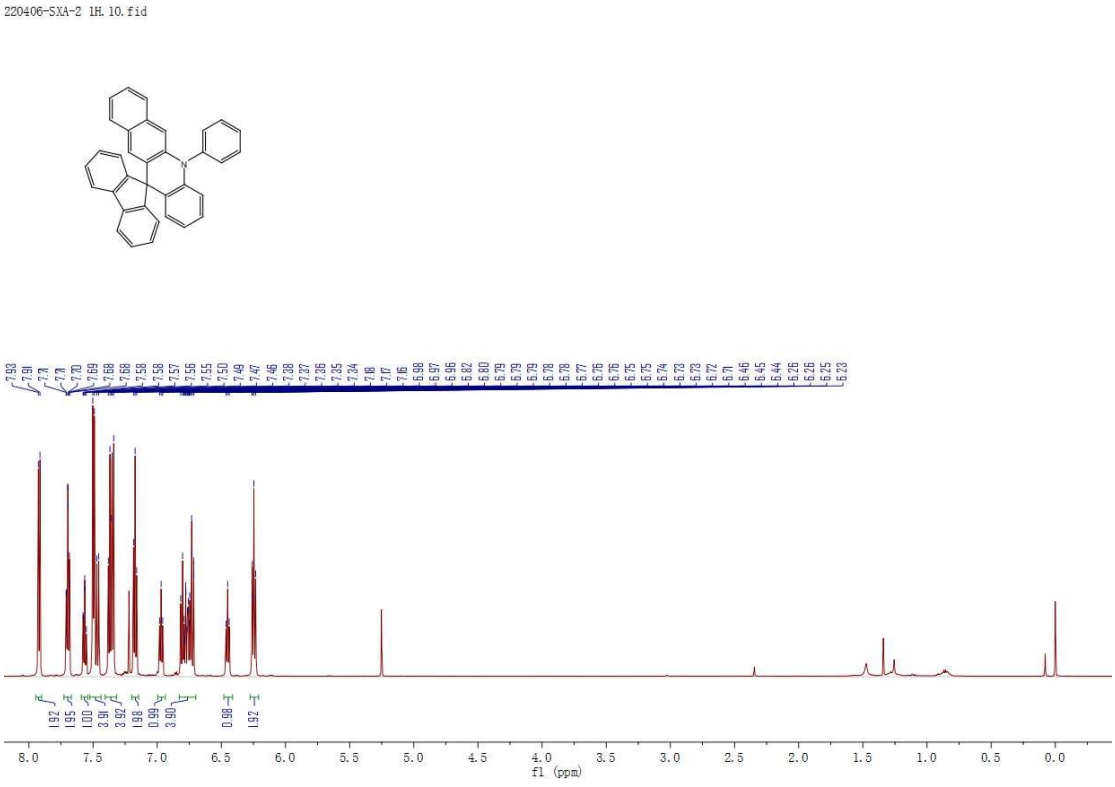

Figure S10 ^{1}H NMR spectrum of SPBAC-BP (400 MHz, $CDCl_3$, 25 °C).

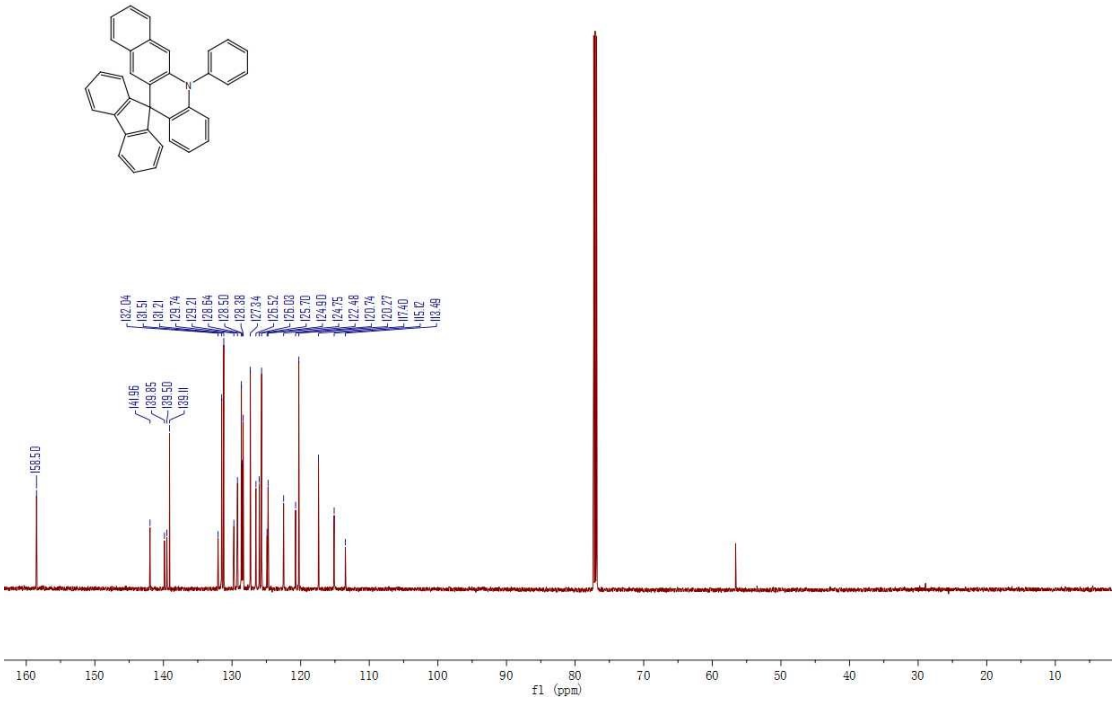

Figure S11 ^{13}C NMR spectrum of SPBAC-BP (400 MHz, $CDCl_3$, 25 °C).

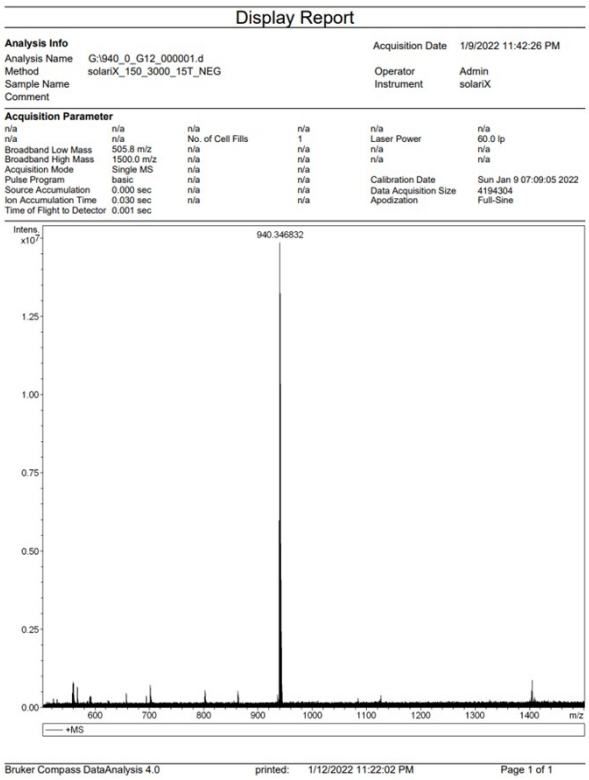

Figure S12 MS of compound SPBAC-BP

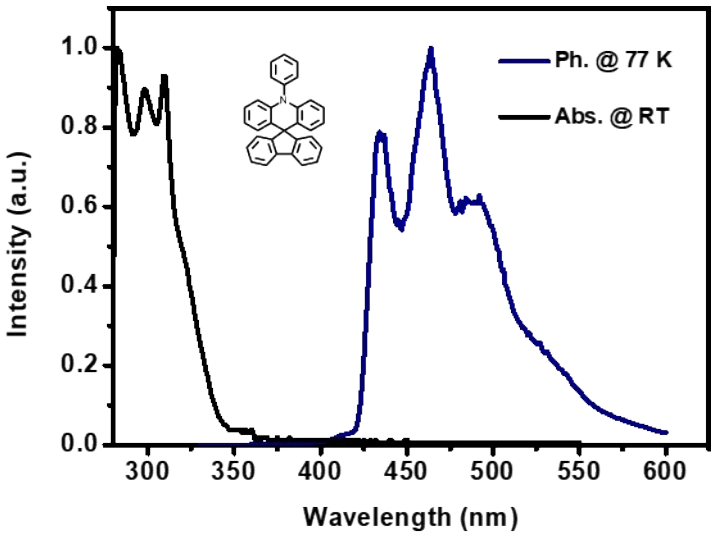

Figure S13 Ultraviolet-visible absorption spectra and phosphorescence spectra of SPAC-PH

Reference

[1] T. Lu, F. Chen, *J. Comput. Chem.* 2012, 33, 580-592.

[2] W. Humphrey, A. Dalke, K. Schulten, *J. Mol. Graphics* 1996, 14, 33-38.